



OPEN

Aberrant static and dynamic functional connectivity of insular cortex in patients with trigeminal neuralgia

Yuying Chen^{1,2,4}, Shumei Li^{2,4}, Meng Li², Linhua Huang², Meien Jiang³, Guomin Li², Jinyan Chen² & Jianhao Yan^{1,2}✉

The abnormal insular-related static and dynamic functional connectivity (sFC and dFC) in patients with trigeminal neuralgia (TN) is not well understood. Therefore, we aimed to explore alterations in the sFC and dFC of the insular cortex (IC) and the relationships between functional connectivity (FC) alterations and clinical measures in TN. The study included 40 patients with TN and 30 healthy controls (HCs) who underwent resting-state functional magnetic resonance imaging and completed the visual analog scale (VAS) and mood questionnaires. Voxel-based sFC and dFC in the bilateral IC were computed. For the voxel-wise FC differences between TN and HC, a two-sample t-test was performed on the individual maps in a voxel-by-voxel manner. To examine linear relationships with clinical measures, Pearson correlations were calculated between FC alterations and VAS and mood measures. Compared with HCs, patients with TN exhibited significantly decreased sFC between the bilateral IC and right superior temporal gyrus, left Rolandic operculum, left thalamus, left supramarginal gyrus, and left superior parietal gyrus, and decreased dFC between the IC and cerebellar vermis. Correlation analysis revealed negative correlations between sFC of IC-thalamus and VAS and dFC of IC-vermis and duration of pain. Our findings reveal brain regions related to pain sensation and regulation showing abnormal sFC and dFC alterations in TN, suggesting their pivotal roles in the neural mechanisms underlying TN.

Keywords Trigeminal neuralgia, Dynamic functional connectivity, Insular cortex, Static functional connectivity, Thalamus

According to the International Headache Society, trigeminal neuralgia (TN) is “a disorder characterized by recurrent episodes of unilateral transient electricity-like pain with sudden onset and termination, limited to the distribution of one or more branches of the trigeminal nerve, and triggered by harmless stimulation.” The estimated incidence of TN is 4.3–26.8 per 100,000 person-years, with a lifetime prevalence of 0.03%–0.3%, and is more common in women than in men^{1,2}. Patients with TN usually have a long disease course, which may result in recurrence of the condition. Consequently, some patients develop anxiety and depressive symptoms, leading to an increased risk of suicide³. Although TN may impose significant personal and social burdens, the underlying neural mechanisms remain unclear.

Recent studies on TN have identified structural and functional abnormalities in brain regions associated with the sensory and cognitive-emotional dimensions of pain, indicating that understanding the changes in the central nervous system may help elucidate the mechanism of TN^{4,5}. Particularly, previous studies have shown that the insular cortex (IC) is a key brain region associated with chronic pain⁶, which is closely related to pain perception^{7,8}. Additionally, recent studies have suggested that structural and functional abnormalities in the IC play important roles in the pathophysiology of TN^{9,10}. Yuan et al. used regional homogeneity (ReHo) analysis to compare abnormal brain function between patients with idiopathic trigeminal neuralgia and healthy groups and found that the ReHo value in patients with idiopathic trigeminal neuralgia mainly decreased in the cerebellum and insula, with ReHo values in the insula negatively correlated with visual analog scale (VAS) scores¹¹. Shen et

¹Guangdong Medical University, Zhanjiang, People's Republic of China. ²Department of Medical Imaging, The Affiliated Guangdong Second Provincial General Hospital of Jinan University, Guangzhou, People's Republic of China. ³Guangzhou University of Traditional Chinese Medicine Shunde Traditional Chinese Medicine Hospital, Foshan, People's Republic of China. ⁴Yuying Chen and Shumei Li have contributed equally to this work. ✉email: yanjianhao@163.com

al. found that the gray matter volume in patients with TN was decreased in multiple brain regions including the bilateral IC at different stages of the disease, with the reduction in the left IC being more pronounced in patients with a longer disease course¹². Similarly, Desouza et al. reported thinning of the ipsilateral dorsal posterior and ventral anterior IC in patients with TN¹³, suggesting that neuropathic pain mainly affected the thickness of the ipsilateral IC. Additionally, we previously found increased regional cerebral blood flow in the left insula region in patients with TN compared with healthy groups, suggesting that it may be related to the processing of negative emotions, pain perception, and pain regulation¹⁴. Although previous studies have shown that local metabolic abnormalities and potential morphological alterations exist in the IC of patients with TN, the changes in functional connectivity (FC) patterns of the IC in patients with TN remain unclear.

Static functional connectivity (sFC) has been extensively employed as a tool to explore the synchronized neural activity occurring between distinct brain regions in a variety of disease states^{15,16}. Therefore, sFC based on region of interest (ROI) is considered a sensitive and reliable method¹⁷ and has been widely used to investigate the alterations in brain function in various chronic pain conditions^{4,18,19}. However, the brain undergoes different states and connections between brain regions change dynamically. Thus, dynamic functional connectivity (dFC) provides a measure of the brain's dynamic features, which can be used to observe the relationship between blood oxygen level dependent (BOLD) signals and brain FC over time. The dFC reveals the pattern of brain activity over time and their relationship with FC, which in turn facilitate sustained neuromodulation of cognition and behavior^{20,21}. Therefore, the understanding of how FC dynamically fluctuates over time can provide critical insights into the neural mechanisms underlying pain processing²². Previous studies utilized dynamic functional approaches to investigate the temporal dynamics of neural circuitry underlying temporal summation of pain in fibromyalgia, providing insights into the neurodynamic mechanisms of central sensitization in this condition²³. Although reports on the use of dFC in TN research remain limited, combining sFC and dFC approaches may provide a more comprehensive understanding of the neuropathological changes underlying TN.

Therefore, this study aimed to explore the alterations of the IC-based sFC and dFC in patients with TN. Furthermore, we aimed to investigate the relationships between abnormal IC-based sFC and dFC and the clinical manifestations of TN. We hypothesized that: (1) patients with TN show abnormal and distinct IC-based sFC and dFC patterns compared with HCs; (2) abnormal IC-based sFC and dFC correlate with the pain intensity and disease duration.

Materials and methods

Participants

Patients with TN were recruited from the Neurosurgery Department of Guangdong Second Province General Hospital between January 2021 and April 2024. All patients with TN were diagnosed according to the International Classification of Headache Disorders (ICHD-III) criteria. The inclusion criteria were: (a) age 18–70 years old; (b) right-handed; (c) no brain trauma or nervous system diseases; (d) no history of alcohol, psychiatric medication intake, or substance abuse; and (e) no magnetic resonance imaging (MRI) contraindications. The exclusion criteria were: (a) chronic pain other than TN nerve-related disease or neuro-related diseases; (b) history of craniocerebral surgery; or (c) MRI contraindications (such as cardiac pacemaker, claustrophobia, or pregnancy).

Overall, 40 patients were enrolled in the study. Basic patient information and disease course were recorded, and neuropathic pain was assessed using the VAS. Patient anxiety- and depression-related symptoms were quantified by a psychiatrist based on the Hamilton Anxiety Scale (HAMA) and the Hamilton Depression Scale (HAMD).

Additionally, 30 age- and sex-matched healthy controls (HCs) were recruited with the following criteria: (a) age 18–70 years old; (b) right-handed; (c) no neurological disease; (d) no alcohol, psychiatric medication intake, or substance abuse; (e) no history of acute or chronic pain during the screening visit; and (f) no MRI contraindications. This study was approved by the Ethics Review Board of Guangdong Second Province General Hospital. All procedures were carried out in accordance with the principles outlined in the 1964 Declaration of Helsinki and its subsequent revisions, as well as in the relevant guidelines. Written informed consent was obtained from all participants.

fMRI data acquisition

Data were acquired using a Philips 3.0 T MRI scanner (Philips Medical Systems, Best, The Netherlands), including resting-state BOLD-fMRI and high-resolution 3D structural images. Participants wore earplugs to minimize scanner noise and lay on the MR machine with the head tightly secured by a foam pad to reduce head movement. During the resting-state fMRI (rs-fMRI) data collection process, all participants were asked to close their eyes while lying down and remain awake without focusing on any particular thought. Participants initially underwent routine MRI examinations to rule out any anatomic abnormalities which were subsequently reviewed by two qualified radiologists to ensure that no organic brain lesions were present. High-resolution 3D brain structure images were obtained using the fast field echo pulse sequence, with the following specific scanning parameters: repetition time (TR)/echo time (TE) = 7.9 ms/3.6 ms; field of view (FOV) = 256 mm × 256 mm; matrix = 256 × 256; flip angle (FA) = 9°; thickness = 1.0 mm (without gap); and 185 transverse slices. Finally, rs-fMRI was performed using a gradient echo planar imaging sequence: TR/TE = 2000 ms/30 ms; FOV = 224 mm × 224 mm; matrix = 64 × 64; FA = 90°; thickness = 3.6 mm; interval = 0.6 mm; interlaced scanning; and 35 transverse slices, collecting a total of 240 phases.

Data preprocessing

All fMRI data were preprocessed using the DPARSF premium version 5.2 (<http://rfmri.org/DPARSF>)²⁴ and MATLAB 2020a (MathWorks, Natick, MA, USA). The first 10 time points of each participant's image were discarded to stabilize the magnetic field and adapt the participants to the scanning environment. Images with

head movement > 2.0 mm or rotation angle $> 2.0^\circ$ were removed to reduce the influence of head movements. The segmentation image toolkit was used for T1 segmentation of white matter, gray matter, and cerebrospinal fluid (CSF). Functional images were registered to structural images and normalized to 3 mm isotropic voxel standard Montreal Neurological Institute (MNI) space. Several nuisance covariates were then removed from the time course of each voxel by linear regression, including the overall mean of the brain, white matter, and CSF signals, and the Friston 24 head motion parameters²⁵. Finally, a bandpass filter (0.01–0.1 Hz) was applied to all images. Images were then smoothed using a 4 mm full-width-at-half-maximum Gaussian kernel, and the trend of linear signal drift was removed.

Head motion

Head motion was computed using Jenkinson's relative root mean square technique²⁶ to remove occurrences of average framewise displacement (FD) during scanning. The mean FD was determined to assess differences in voxel motion between the two groups. No significant difference in average FD was observed between the TN and HC groups ($P = 0.89$).

Static and dynamic functional connectivity

Based on the automated anatomical labeling (AAL) map in the DPARSF 5.2 (<http://rfmri.org/dpabi>), the bilateral IC (areas 29 and 30) was extracted as the ROI. The sFC was performed by calculating the average time series of the bilateral IC and other brain regions, which were then transformed using Fisher's *r*-to-*z* transformation to fit a normal distribution for statistical analysis.

The sliding window analysis²⁷, which divides the entire fMRI scan into data segments and calculates the temporal correlation for each segment, is the most popular method used to estimate dFC. The length of the window is a crucial parameter, as it determines the tradeoff between time resolution and estimation accuracy²⁸. A small window size yields improved capability to track fast the temporal changes but at the cost of introducing spurious fluctuations and increased sensitivity to noise²⁹. Accordingly, several studies have shown that a window length of 50 TR is suitable for maintaining a balance between achieving reliable FC calculations and capturing time-varying variations in high-speed FC^{30–32}. Therefore, the sliding window was set to 50 TR (100 s) with a step size of 2 TR (4 s)^{33,34} to calculate the correlation coefficient between the ROI for each window and the brain voxel, followed by Fisher *Z*-transformation to improve normality. The variance in FC within each time window for each participant was calculated, which provided an FC variance map. A two-sample *t*-test was performed to compare differences between the TN and HC groups (two-tailed, voxel-level $P < 0.001$, Gaussian random field (GRF) correction, cluster-level $P < 0.05$).

The GRF method was employed for multiple comparison corrections to control the false positive rate and guarantee the statistical credibility of the results. The GRF method is based on the spatial random field theory, which considers the spatial correlation among voxels by assessing the smoothness of statistical images and calculates the significance threshold^{24,35}. Specifically, we first generated statistical images reflecting the correlations of brain regions and then used GRF for multiple comparisons to correct the smoothness of these images, setting voxel-level $P < 0.001$ and cluster-level $P < 0.05$. This process ensures that the significant results detected are strictly corrected, effectively avoiding misjudgments caused by multiple comparisons.

Statistical analysis

The SPSS 25.0 software (IBM Corp., Armonk, NY, USA) was used to conduct a two-sample, two-tailed *t*-test to evaluate differences in age and years of education between patients with TN and HCs. Sex composition between the two groups was assessed using the Chi-square test. A two-sample *t*-test was performed on the individual *z*-transformed IC-based sFC and dFC to assess voxel-wise differences in IC-based sFC and dFC between HCs and patients with TN. The multiple comparison correction was performed using GRF corrected voxel-level $P < 0.001$ and cluster-level $P < 0.05$. Pearson's correlation analysis was performed to assess the correlation between abnormal IC-based sFC and dFC and duration of pain, VAS, HAMA, and HAMD scores with age, sex and education level as covariables.

Results

Demographic and clinical characteristics

The demographic characteristics of patients with TN and HCs were presented in Table 1. No significant differences were observed in age, sex and education level between the patients with TN and HCs. The mean duration of pain for the TN group was 5.70 years.

Alterations of IC-based sFC in patients with TN and correlations with VAS

Compared with HCs, patients with TN showed decreased sFC between the bilateral IC and right superior temporal gyrus (STG), left Rolandic operculum, left thalamus, left supramarginal gyrus, and left superior parietal gyrus (Table 2, Fig. 1). Correlation analysis revealed that sFC between IC-left thalamus in patients with TN was negatively correlated with VAS ($R = -0.372$, $P = 0.018$) (Fig. 2). However, no significant correlations were observed between the remaining abnormal IC-based sFC and the clinical measurements (Table 2).

Alterations of insular-based dFC in patients with TN and correlation with duration of pain

Compared with the HC group, the dFC of IC-vermis was reduced in patients with TN (Table 3). Partial correlation analysis showed that dFC of IC-vermis was significantly negatively correlated with the duration of pain ($R = -0.315$, $P = 0.048$) (Fig. 3).

Characteristic	TN (N=40)	HC (N=30)	P value
Age (y)	57.00 (48.25,61.75)	55.50 (53.00, 61.00)	0.986 ^a
Sex (F/M)	29/11	19/11	0.414 ^b
Education (Y)	9.00 (6.00,12.00)	12.00 (6.00,16.00)	0.136 ^a
Affected side (L/R)	10/30	/	/
Duration of pain (years)	5.70 ± 5.78	/	/
VAS score	6.98 ± 1.40	/	/
HAMA score	10.08 ± 5.65	/	/
HAMD score	9.40 ± 5.71	/	/

Table 1. Demographic characteristics of patients with TN and the healthy controls (HCs). TN, trigeminal neuralgia; HC, healthy control; VAS, visual analog scale; HAMD, Hamilton Depression Rating Scale; HAMA, Hamilton Anxiety Rating Scale. Demographic data that follow normal distribution are shown as mean ± standard deviation. Demographic data of non-normal distribution are shown as a median (quartile spacing). ^aP-value was obtained by the Mann–Whitney U test. ^bP-value was obtained by the chi-square test. /: not applicable.

Cluster	Brain region	Cluster size	MNI			T value
			x	y	z	
Cluster1	SupraMarginal_L	121	−54	−24	18	−3.456
Cluster2	Temporal_Sup_R	114	63	−3	−9	−3.457
Cluster3	Thalamus_L	100	−11	−20	16	−3.453
Cluster4	Parietal_Sup_L	83	−36	−78	39	−3.449
Cluster5	Temporal_Sup_R	82	69	−27	12	−3.449
Cluster6	Rolandic_Oper_L	60	−51	0	9	−3.457

Table 2. Brain regions showing significantly reduced IC-based sFC in patients with TN. MNI, Montreal Neurological Institute; L, left; R, right. Two-sample t-test, Two-Tailed, Voxel-Level $P < 0.001$, GRF Correction, Cluster-Level $P < 0.05$.

Discussion

In the current study, we investigated the IC-based sFC and dFC in patients with TN and explored the correlations between altered IC-based sFC/dFC with clinical features. We found reduced IC-based sFC mainly in the right STG, left Rolandic operculum, left thalamus, left supramarginal gyrus, and left superior parietal gyrus in patients with TN. Whereas, reduced IC-based dFC was only found in cerebellar vermis in patients with TN. Further analysis revealed negative correlations between sFC of the IC-thalamus and VAS as well as between dFC in IC-vermis and duration of pain. Thus, our findings reveal the altered and distinct IC-based sFC and dFC patterns in patients with TN, with brain regions related to pain sensation and regulation showing abnormal sFC and dFC alterations. The significant correlations between the IC-based sFC/dFC with VAS pain scores and duration of pain suggest the pivotal role of IC in the neural mechanisms underlying TN.

Our first notable finding is the reduced sFC in the IC-left thalamus, which suggests decreased synchronization between the two key regions involved in pain processing. Although the exact mechanism underlying TN remains to be further elucidated, the central role of the thalamus, as a key relay station transmitting pain signals to the cerebral cortex, in the pathogenesis of TN has been demonstrated³⁶. Some previous studies have also reported abnormal thalamic function in patients with TN^{33,37}. Particularly, in our previous studies on BOLD-fMRI for TN, we reported an increase in the dynamic ReHo value³³ and regional cerebral blood flow value¹⁴ in the thalamus of patients with TN, which was positively correlated with the duration of pain. Collectively, these previous studies suggest the important role of thalamic spontaneous nerve activity and local hemodynamics in the pathogenesis of TN. Additionally, Martinelli et al. induced migraine attacks using nitroglycerin and found that FC changes between the right thalamus and insula during the prodromal phase peaked during the full-blown phase³⁸. However, our results contradict those of a previous study³⁹, which reported that the FC between the insula and thalamus was abnormally increased in patients with TN. A plausible explanation for the significant difference in pain intensity associated with TN between the current study (averaging 6.98 ± 1.40) and previous research (averaging 2.3 ± 1.41) could be the varying severity of TN among participants. We hypothesize that alterations in the FC between the IC and thalamus in TN follow two distinct stages. Initially, when TN pain intensity is mild, hyper-connectivity (hyper-FC) between the IC and thalamus emerges as a compensatory mechanism, potentially facilitating increased communication between these regions to manage the pain. However, as the pain intensity intensifies and becomes severe, we speculate that FC between the IC and thalamus decreases, suggesting a shift in neural processing strategies or the exhaustion of compensatory mechanisms. Importantly, our study revealed a significant negative correlation between pain intensity and insular-thalamus FC in TN patients, further emphasizing the potential role of this neural pathway in TN pathogenesis. This

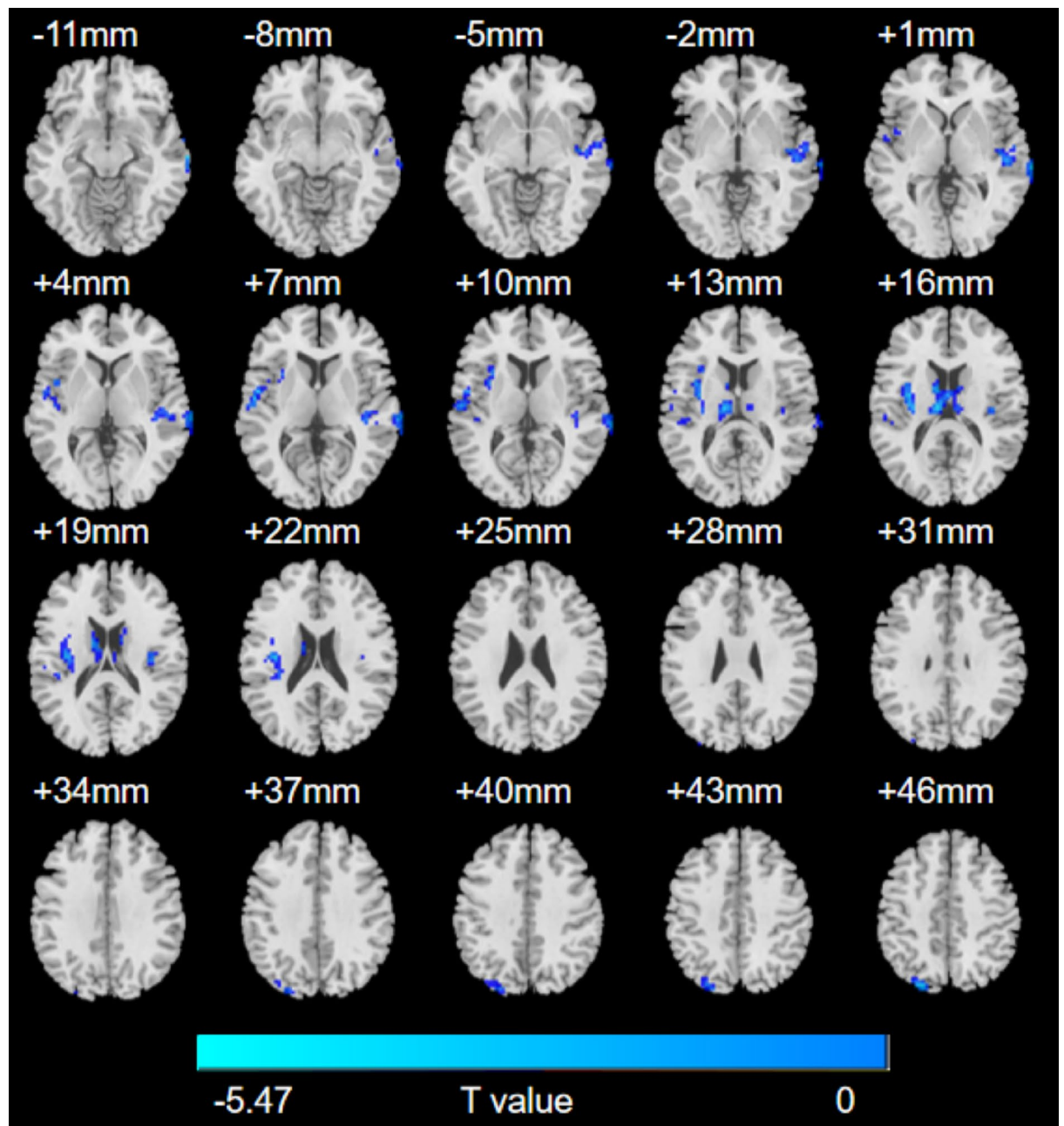


Fig. 1. Between group voxel-based comparisons of IC-based zsFC maps. The significant brain regions show reduced IC-based zsFC in patients with TN is presented in axial map from $Z = -11$ to $Z = +46$ mm (every 3 mm). Cool colors represent decreased connectivity in the TN patient group.

discovery indicates that the synchronization between the IC and the thalamus decreases as the intensity of pain experienced by patients increases, potentially reflecting the brain's decreasing capacity to adaptively respond to increasing pain. The involvement of insula in modulating emotional responses to pain suggests that a decrease in its FC with the thalamus could lead to a diminished ability to regulate distress and anxiety associated with pain, thereby intensifying the patient's perception of pain. Additionally, these changes in sFC might indicate neural fatigue or the exhaustion of compensatory mechanisms that may have initially emerged to manage lower pain levels. Nevertheless, further investigation of this theory is required to fully understand the dynamic changes in neural connectivity that occur in response to varying degrees of TN pain⁴⁰.

Our study also identified abnormal sFC between the IC and the STG. This is consistent with previous studies on chronic pain which reported that the temporal lobe is involved in pain perception^{41,42}. Guarnera et al.⁴³ investigated early changes in cortical thickness in children with migraine without aura and found that the cortical thickness in the STG and posterior insula in patients over 12 years old was reduced compared to younger patients. This suggests that the STG is involved in pain processing by supervising the mismatch between pain anticipation and pain perception and regulating pain expression, illustrating the key role of insula in chronic

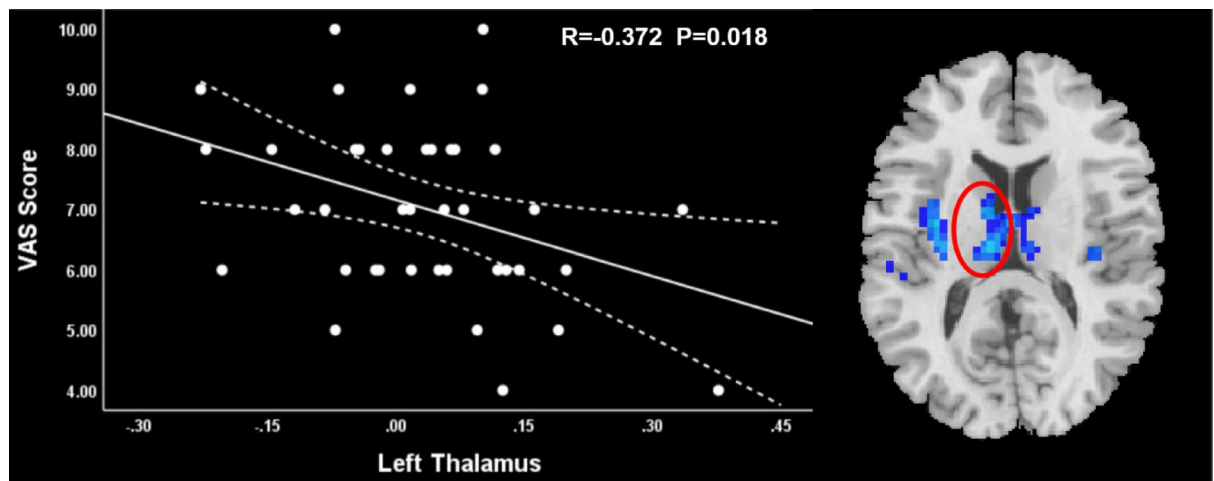


Fig. 2. Significant negative correlation between IC-left thalamus sFC and VAS score in patients with TN.

Brain region	Cluster size	MNI			T value
		x	y	z	
Vermis	37	0	-54	-21	-2.659

Table 3. Brain regions showing reduced IC-based dFC in patients with TN compared with healthy controls (HCs). MNI, Montreal Neurological Institute. Two-sample t-test, Two-Tailed, Voxel-Level $P < 0.01$, GRF Correction, Cluster-Level $P < 0.05$.

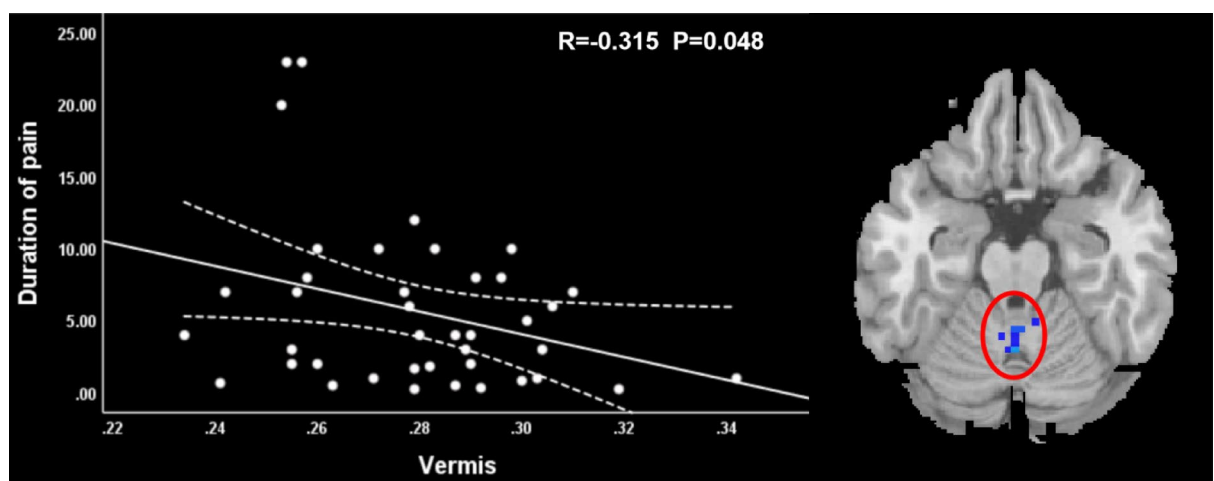


Fig. 3. Significant negative correlation between dFC of IC-vermis and duration of pain in patients with TN.

pain and nociceptive networks. Our findings further demonstrate a reduction in sFC between the IC and STG, providing additional evidence to support the important role of the STG plays in pain regulation.

We observed reduced sFC between the IC and supramarginal gyrus in patients with TN. The supramarginal gyrus is part of the inferior parietal lobule and belongs to the default mode network (DMN)⁴⁴. The DMN plays an important role in self-reference, social cognition, autobiographical memory, and language. The DMN is activated when a person is not engaged in a task. Zhang et al.⁴⁵ explored changes in sFC between the insula and brain regions in DMN in patients with low back pain and found that FC between the insula and the inferior parietal lobule was significantly reduced in pain, suggesting that pain may disrupt the functional connections between the insula and inferior parietal lobule which belongs to the DMN. Similarly, we observed reduced functional connections between the IC and the supramarginal gyrus in patients with TN, suggesting that pain may inhibit activation of the DMN, leading to its dysfunction.

Reduced functional connections between the IC and left superior parietal gyrus in patients with TN were observed in the present study. The parietal cortex has long been recognized as a site for sensorimotor integration and is involved in pain sensations and painful emotions^{46–48}. A previous study have also suggested that the parietal gyrus may be involved in analgesia, and its stimulation may influence the judgment of pain intensity and reduce the perception of pain intensity⁴⁹. Changes in the function and structure of the superior parietal gyrus have also been found in TN and other chronic pain diseases^{33,50,51}. Jin et al. found that the functional connection between the periaqueductal gray and superior parietal gyrus in patients with primary dysmenorrhea was reduced during the pain period, indicating a disorder in the descending pain regulation system⁵², that affects patient's pain perception. Therefore, we hypothesized that the decreased FC between the IC and superior parietal gyrus, observed in this study, may relate to pain perception dysfunction in patients with TN.

We also observed reduced functional connections between the IC and the Rolandic operculum. Previous researchers used high-frequency electrical stimulation to test brain responses and found that the oropharyngeal response was the most common when the Rolandic operculum was stimulated, with a quarter of the oropharyngeal sensations associated with dysarthria⁵³. Jezzini et al. used intracortical microstimulation to stimulate monkeys with a low-impedance tungsten microelectrode and found a strong connection pattern between the insula and the Rolandic operculum, supporting the integration of sensory and taste information for effective eating behavior⁵⁴. Therefore, we speculate that the decreased functional connection between the IC and Rolandic operculum may be related to the incoordination or rigidity of oral muscles in patients with TN, resulting in slurred speech, dysphonia, and decreased appetite.

Our dFC analysis revealed reduced dFC in the IC and cerebellum vermis in patients with TN. A consensus paper on ataxic gait stated⁵⁵ that “the vermis of the cerebellum is essential for postural control”. Cerebellar ataxia is characterized by postural and gait abnormalities, voluntary motor coordination disorders, speech disorders, eye movement disorders, and decreased muscle tone. Reyes et al. explored the effects of botulinum toxin A on neural activity in brain regions related to pain in patients with chronic eye pain and found that after botulinum toxin A injection, neural activity decreased in brain regions associated with motor aspect of pain, including the cerebellar vermis and bilateral cerebellar lobule VI⁵⁶. Thus, patients with TN may be more prone to feeling pain in certain positions. Therefore, they may choose to avoid these positions, gradually developing poor body posture. Additionally, in this study, the reduction of dFC between the IC and vermis in patients with TN was negatively correlated with the duration of pain, suggesting that longer disease progression is associated with weaker coupling between the IC and vermis. The IC is important in pain perception and interoceptive processing, while the cerebellar vermis plays a crucial role in postural control and motor coordination. The observed decrease in dFC between the IC and vermis might reflect a decline in functional integration, potentially representing maladaptive neuroplastic alterations that impair the neural circuits mediating the integration of nociceptive signals with motor and postural regulation. Therefore, the significant negative correlation between dFC of IC-vermis and duration of pain might indicate that weakened IC-vermis dFC impairs the brain's ability to modulate pain through adaptive motor strategies (e.g., smooth postural adjustments), leading to further reliance on maladaptive compensatory behaviors.

Additionally, we observed distinct pattern differences in insular-based sFC and dFC, indicating that these two measures might complement each other in elucidating neural biology in TN. The sFC provides baseline status information of brain functional networks, while the dFC reveals dynamic changes under different states. Furthermore, widespread alterations detected in insular-based sFC across multiple brain regions suggest that the sFC could more effectively capture subtle neuronal changes associated with TN compared to dFC. This highlights the potential value of both measures in comprehensively elucidating TN's neural mechanisms.

Despite the notable results, this study has some limitations that must be considered. First, since this study was not longitudinal, we were unable to determine a causal relationship between functional abnormalities and TN development. Second, the sample size was relatively small, which may have affected the accuracy of the results. Consequently, further studies with larger sample sizes are warranted to validate the results of our present study. Third, uneven distribution of the affected side (left 10/right 30) may have led to a left lateralization of outcomes, which may indicate neurological adaptation or possible compensatory changes. Thus, future studies should consider the effects on the affected side. Finally, all patients with TN in this study were taking pain medications, therefore, we cannot rule out possible confounding effects of medications on FC analysis.

Conclusions

In conclusion, our findings underscore the presence of abnormal alterations in both sFC and dFC within brain regions central to pain sensation and regulation in patients with TN. Notably, the observed abnormal sFC between the IC and the thalamus, along with its significant negative correlation with VAS pain scores, implicates the pivotal role of sFC abnormalities in IC-thalamus in the pathophysiology of TN. Furthermore, the significant reduction in dFC between the IC and the vermis of the cerebellum, which also displays a significant negative association with disease duration, suggests that dynamic changes in FC patterns may serve as markers of disease progression or chronicity. Collectively, these results deepen our understanding of the neural mechanisms underlying TN, highlighting the importance of disrupted functional integration among key brain regions involved in pain processing and modulation.

Data availability

The data that support the findings of this study are not openly available due to reasons of sensitivity and are available from the corresponding author upon reasonable request.

Received: 10 October 2024; Accepted: 16 June 2025

Published online: 01 July 2025

References

- De Toledo, I. P. et al. Prevalence of trigeminal neuralgia. *J. Am. Dent. Assoc.* **147**, 570–576.e572. <https://doi.org/10.1016/j.adaj.2016.02.014> (2016).
- Mueller, D. et al. Prevalence of trigeminal neuralgia and persistent idiopathic facial pain: A population-based study. *Cephalal. Int. J. Headache* **31**, 1542–1548. <https://doi.org/10.1177/0333102411424619> (2011).
- Araya, E. I., Claudino, R. F., Piovesan, E. J. & Chichorro, J. G. Trigeminal neuralgia: Basic and clinical aspects. *Curr. Neuroparmacol.* **18**, 109–119. <https://doi.org/10.2174/1570159x17666191010094350> (2020).
- Tsai, Y. H. et al. Altered structure and functional connection in patients with classical trigeminal neuralgia. *Hum. Brain Mapp.* **39**, 609–621. <https://doi.org/10.1002/hbm.23696> (2018).
- Wang, Y. et al. Altered brain structure and function associated with sensory and affective components of classic trigeminal neuralgia. *Pain* **158**, 1561–1570. <https://doi.org/10.1097/j.pain.0000000000000951> (2017).
- Yarkoni, T., Poldrack, R. A., Nichols, T. E., Van Essen, D. C. & Wager, T. D. Large-scale automated synthesis of human functional neuroimaging data. *Nat. Methods* **8**, 665–670. <https://doi.org/10.1038/nmeth.1635> (2011).
- Bushnell, M. C., Ceko, M. & Low, L. A. Cognitive and emotional control of pain and its disruption in chronic pain. *Nat. Rev. Neurosci.* **14**, 502–511. <https://doi.org/10.1038/nrn3516> (2013).
- Lu, C. et al. Insular cortex is critical for the perception, modulation, and chronification of pain. *Neurosci. Bull.* **32**, 191–201. <https://doi.org/10.1007/s12264-016-0016-y> (2016).
- Mammadkhanli, O., Niftaliyev, S. & Simsek, O. Involvement of the cingulate cortex and insula in patients with trigeminal neuralgia: A clinical and volumetric study. *Clin. Neurol. Neurosurg.* **243**, 108394. <https://doi.org/10.1016/j.clineuro.2024.108394> (2024).
- Liu, W. C. et al. Neural activity in trigeminal neuralgia patients with sensory and motor stimulations: A pilot functional MRI study. *Clin. Neurol. Neurosurg.* **219**, 107343. <https://doi.org/10.1016/j.clineuro.2022.107343> (2022).
- Yuan, J. et al. Altered spontaneous brain activity in patients with idiopathic trigeminal neuralgia: A resting-state functional mri study. *Clin. J. Pain* **34**, 600–609. <https://doi.org/10.1097/ajp.0000000000000578> (2018).
- Shen, S. et al. Gray matter volume reduction with different disease duration in trigeminal neuralgia. *Neuroradiology* **64**, 301–311. <https://doi.org/10.1007/s00234-021-02783-y> (2022).
- Desouza, D. D., Moayed, M., Chen, D. Q., Davis, K. D. & Hodaie, M. Sensorimotor and pain modulation brain abnormalities in trigeminal neuralgia: A paroxysmal, sensory-triggered neuropathic pain. *PLoS ONE* **8**, e66340. <https://doi.org/10.1371/journal.pone.0066340> (2013).
- Zhou, Q. et al. Cerebral perfusion alterations in patients with trigeminal neuralgia as measured by pseudo-continuous arterial spin labeling. *Front. Neurosci.* **16**, 1065411. <https://doi.org/10.3389/fnins.2022.1065411> (2022).
- Wang, T. et al. Increased insular connectivity with emotional regions in primary insomnia patients: A resting-state fMRI study. *Eur. Radiol.* **27**, 3703–3709. <https://doi.org/10.1007/s00330-016-4680-0> (2017).
- Mills, E. P. et al. Brainstem pain-control circuitry connectivity in chronic neuropathic pain. *J. Neurosci.* **38**, 465–473. <https://doi.org/10.1523/jneurosci.1647-17.2017> (2018).
- Hampson, M., Peterson, B. S., Skudlarski, P., Gatenby, J. C. & Gore, J. C. Detection of functional connectivity using temporal correlations in MR images. *Hum. Brain Mapp.* **15**, 247–262. <https://doi.org/10.1002/hbm.10022> (2002).
- Schwedt, T. J. et al. Allodynia and descending pain modulation in migraine: a resting state functional connectivity analysis. *Pain Med. Malden, Mass.* **15**, 154–165. <https://doi.org/10.1111/pme.12267> (2014).
- Zhang, C. et al. Alterations in functional connectivity in patients with non-specific chronic low back pain after motor control exercise: a randomized trial. *Eur. J. Phys. Rehabil. Med.* **60**, 319–330. <https://doi.org/10.23736/s1973-9087.24.08087-0> (2024).
- Preti, M. G., Bolton, T. A. & Van De Ville, D. The dynamic functional connectome: State-of-the-art and perspectives. *Neuroimage* **160**, 41–54. <https://doi.org/10.1016/j.neuroimage.2016.12.061> (2017).
- Hutchison, R. M. et al. Dynamic functional connectivity: promise, issues, and interpretations. *Neuroimage* **80**, 360–378. <https://doi.org/10.1016/j.neuroimage.2013.05.079> (2013).
- Necka, E. A. et al. Applications of dynamic functional connectivity to pain and its modulation. *Pain Rep.* **4**, e752. <https://doi.org/10.1097/pr9.0000000000000752> (2019).
- Cheng, J. C. et al. Dynamic functional brain connectivity underlying temporal summation of pain in fibromyalgia. *Arthr. Rheumatol.* **74**, 700–710. <https://doi.org/10.1002/art.42013> (2022).
- Yan, C. G., Wang, X. D., Zuo, X. N. & Zang, Y. F. DPABI: Data processing & analysis for (resting-state) brain imaging. *Neuroinformatics* **14**, 339–351. <https://doi.org/10.1007/s12021-016-9299-4> (2016).
- Friston, K. J., Williams, S., Howard, R., Frackowiak, R. S. & Turner, R. Movement-related effects in fMRI time-series. *Magn. Reson. Med.* **35**, 346–355. <https://doi.org/10.1002/mrm.1910350312> (1996).
- Jenkinson, M., Bannister, P., Brady, M. & Smith, S. Improved optimization for the robust and accurate linear registration and motion correction of brain images. *Neuroimage* **17**, 825–841. [https://doi.org/10.1016/s1053-8119\(02\)91132-8](https://doi.org/10.1016/s1053-8119(02)91132-8) (2002).
- Kiviniemi, V. et al. A sliding time-window ICA reveals spatial variability of the default mode network in time. *Brain Connect.* **1**, 339–347. <https://doi.org/10.1089/brain.2011.0036> (2011).
- Savva, A. D., Mitsis, G. D. & Matsopoulos, G. K. Assessment of dynamic functional connectivity in resting-state fMRI using the sliding window technique. *Brain Behav.* **9**, e01255. <https://doi.org/10.1002/brb3.1255> (2019).
- Shakil, S., Billings, J. C., Keilholz, S. D. & Lee, C. H. Parametric dependencies of sliding window correlation. *IEEE Trans. Biomed. Eng.* **65**, 254–263. <https://doi.org/10.1109/tbme.2017.2762763> (2018).
- Liu, J. et al. Temporal variability of regional intrinsic neural activity in drug-naïve patients with obsessive-compulsive disorder. *Hum. Brain Mapp.* **42**, 3792–3803. <https://doi.org/10.1002/hbm.25465> (2021).
- Cui, G. et al. Static and dynamic functional connectivity of the prefrontal cortex during resting-state predicts self-serving bias in depression. *Behav. Brain Res.* **379**, 112335. <https://doi.org/10.1016/j.bbr.2019.112335> (2020).
- Luo, Q. et al. Aberrant static and dynamic functional connectivity of amygdala subregions in patients with major depressive disorder and childhood maltreatment. *NeuroImage Clin.* <https://doi.org/10.1016/j.nicl.2022.103270> (2022).
- Yan, J. et al. Alterations of dynamic regional homogeneity in trigeminal neuralgia: A resting-state fMRI study. *Front. Neurol.* **10**, 1083. <https://doi.org/10.3389/fneur.2019.01083> (2019).
- Ge, X. et al. Altered brain function in classical trigeminal neuralgia patients: ALFF, ReHo, and DC static- and dynamic-frequency study. *Cereb. Cortex* <https://doi.org/10.1093/cercor/bhad455> (2024).
- Bennett, C. M., Wolford, G. L. & Miller, M. B. The principled control of false positives in neuroimaging. *Social Cogn. Affect. Neurosci.* **4**, 417–422. <https://doi.org/10.1093/scan/nsp053> (2009).
- Groh, A., Krieger, P., Mease, R. A. & Henderson, L. Acute and chronic pain processing in the thalamocortical system of humans and animal models. *Neuroscience* **387**, 58–71. <https://doi.org/10.1016/j.neuroscience.2017.09.042> (2018).
- Wang, Y. et al. Altered regional homogeneity of spontaneous brain activity in idiopathic trigeminal neuralgia. *Neuropsychiatr. Dis. Treat.* **11**, 2659–2666. <https://doi.org/10.2147/ndt.S94877> (2015).
- Martinelli, D. et al. Thalamocortical connectivity in experimentally-induced migraine attacks: A pilot study. *Brain Sci.* <https://doi.org/10.3390/brainsci11020165> (2021).

39. Wang, Y. et al. Structural and functional abnormalities of the insular cortex in trigeminal neuralgia: A multimodal magnetic resonance imaging analysis. *Pain* **159**, 507–514. <https://doi.org/10.1097/j.pain.0000000000001120> (2018).
40. Peltz, E. et al. Functional connectivity of the human insular cortex during noxious and innocuous thermal stimulation. *Neuroimage* **54**, 1324–1335. <https://doi.org/10.1016/j.neuroimage.2010.09.012> (2011).
41. Smallwood, R. F. et al. Structural brain anomalies and chronic pain: a quantitative meta-analysis of gray matter volume. *J. Pain* **14**, 663–675. <https://doi.org/10.1016/j.jpain.2013.03.001> (2013).
42. Rottmann, S., Jung, K., Vohn, R. & Ellrich, J. Long-term depression of pain-related cerebral activation in healthy man: An fMRI study. *Eur. J. Pain* **14**, 615–624. <https://doi.org/10.1016/j.ejpain.2009.10.006> (2010).
43. Guarnera, A. et al. Early alterations of cortical thickness and gyrification in migraine without aura: A retrospective MRI study in pediatric patients. *J. Headache Pain* **22**, 79. <https://doi.org/10.1186/s10194-021-01290-y> (2021).
44. Menon, V. 20 years of the default mode network: A review and synthesis. *Neuron* **111**, 2469–2487. <https://doi.org/10.1016/j.neuron.2023.04.023> (2023).
45. Zhang, S. et al. Resting-state connectivity in the default mode network and insula during experimental low back pain. *Neural Regen. Res.* **9**, 135–142. <https://doi.org/10.4103/1673-5374.125341> (2014).
46. May, A. Structural brain imaging: A window into chronic pain. *The Neurosci.* **17**, 209–220. <https://doi.org/10.1177/1073858410396220> (2011).
47. Derbyshire, S. W. A systematic review of neuroimaging data during visceral stimulation. *Am. J. Gastroenterol.* **98**, 12–20. <https://doi.org/10.1111/j.1572-0241.2003.07168.x> (2003).
48. Ma, J. et al. Alterations in brain structure and function in patients with osteonecrosis of the femoral head: A multimodal MRI study. *PeerJ* **9**, e11759. <https://doi.org/10.7717/peerj.11759> (2021).
49. Valmunen, T. et al. Modulation of facial sensitivity by navigated rTMS in healthy subjects. *Pain* **142**, 149–158. <https://doi.org/10.1016/j.pain.2008.12.031> (2009).
50. Wang, Z. W. et al. Brain structural and functional changes during menstrual migraine: Relationships with pain. *Front. Mol. Neurosci.* **15**, 967103. <https://doi.org/10.3389/fnmol.2022.967103> (2022).
51. Bu, C. et al. Alteration of static and dynamic intrinsic brain activity induced by short-term spinal cord stimulation in postherpetic neuralgia patients. *Front. Neurosci.* **17**, 1254514. <https://doi.org/10.3389/fnins.2023.1254514> (2023).
52. Jin, P. et al. Revealing the mechanism of central pain hypersensitivity in primary dysmenorrhea: Evidence from neuroimaging. *Quant. Imaging Med. Surg.* **14**, 3075–3085. <https://doi.org/10.21037/qims-23-1687> (2024).
53. Mäliä, M. D. et al. Functional mapping and effective connectivity of the human operculum. *Cortex* **109**, 303–321. <https://doi.org/10.1016/j.cortex.2018.08.024> (2018).
54. Jezzini, A., Caruana, F., Stoianov, I., Gallese, V. & Rizzolatti, G. Functional organization of the insula and inner perisylvian regions. *Proc. Natl. Acad. Sci. U.S.A.* **109**, 10077–10082. <https://doi.org/10.1073/pnas.1200143109> (2012).
55. Cabaraux, P. et al. Consensus paper: Ataxic gait. *Cerebellum (London, England)* **22**, 394–430. <https://doi.org/10.1007/s12311-022-01373-9> (2023).
56. Reyes, N. et al. Botulinum toxin A decreases neural activity in pain-related brain regions in individuals with chronic ocular pain and photophobia. *Front. Neurosci.* **17**, 1202341. <https://doi.org/10.3389/fnins.2023.1202341> (2023).

Acknowledgements

The author would like to thank Editage for technical editing of the manuscript.

Author contributions

Y.C. and S.L. wrote the main manuscript text. L.H., G.L., and J.C. collected participants' data. M.J. offered help with formal analysis. M.L. and J.Y. reviewed and edited the manuscript. All authors reviewed the manuscript.

Funding

This study was funded by the National Natural Scientific Foundation of China (81901731), the Science and Technology Program of Guangzhou (No. 2023A03J0760, 2024A03J0856, 2025A03J4294), and Lift Project Foundation of Guangdong Second Provincial General Hospital (TJGC-2025003).

Declarations

Competing interest

The authors declare no competing interests.

Ethical approval

The studies involving human participants were reviewed and approved by the Medical Ethics Committee of Guangdong Second Provincial General Hospital. The patients/participants provided their written informed consent to participate in this study.

Additional information

Correspondence and requests for materials should be addressed to J.Y.

Reprints and permissions information is available at www.nature.com/reprints.

Publisher's note Springer Nature remains neutral with regard to jurisdictional claims in published maps and institutional affiliations.

Open Access This article is licensed under a Creative Commons Attribution-NonCommercial-NoDerivatives 4.0 International License, which permits any non-commercial use, sharing, distribution and reproduction in any medium or format, as long as you give appropriate credit to the original author(s) and the source, provide a link to the Creative Commons licence, and indicate if you modified the licensed material. You do not have permission under this licence to share adapted material derived from this article or parts of it. The images or other third party material in this article are included in the article's Creative Commons licence, unless indicated otherwise in a credit line to the material. If material is not included in the article's Creative Commons licence and your intended use is not permitted by statutory regulation or exceeds the permitted use, you will need to obtain permission directly from the copyright holder. To view a copy of this licence, visit <http://creativecommons.org/licenses/by-nc-nd/4.0/>.

© The Author(s) 2025